
CHAPTER 3 METHOD OF EXPERIMENTATION AND ANALYSIS

3.1 INTRODUCTION

This chapter presents the evaluation of the current theory with specific emphasis on the data that needed to be collected from working shafts to validate the theory for calculating pressure drops over shafts.

Thereafter, the manner in which the initial tests were conducted and the conclusions drawn from these tests are discussed. The specific outcome of this chapter is to validate the theory (as noted above), as well as to define a testing methodology for use on the remainder of the shafts to be tested.

The tests completed on various shafts are discussed and the relevance of the results is noted.

The final section consists of the CFD modelling of the selected shaft sections and the calibration of the model such that these sections can be accurately reflected. These models are then used to determine the various pressure loss components and the potential for modifying the current use of these components to reduce the overall pressure resistance that shafts offer to the ventilation air flowing through them.

3.2 THEORY FOR ANALYSIS OF SHAFT RESISTANCES

3.2.1 Static Resistance of Shafts

To calculate the expected pressure drop in a shaft, standard analysis techniques are used. The background and development of this theory was discussed in more detail in CHAPTER 2. Three different methods are used for the calculation of shaft friction resistances. All these methods are similar and are based on the same data produced by Stevenson (1956), whose work was later extrapolated and defined by Bromilov (1960) and McPherson (1987).

The methods referred to are:

- 1 Classic fluid dynamics theory using the Chezy-Darcy friction factors and the Darcy-Weisbach approach (White, 1986)
- 2 General mine ventilation approach using the Atkinson equation and friction calculations (Hemp, 1979, 1989)

3 The rational resistance theory as laid down by McPherson (1987)

Each of these methods is discussed in turn in the following sections.

3.2.1.1 Chezy-Darcy friction factor

The resistance that ducts offer to the flow of fluid through them is calculated using the Chezy-Darcy friction factor (f). This factor is used to calculate the pressure drop over a length of duct. It is valid for duct flows of any cross-section, as well as for laminar and turbulent flow. The manner in which this pressure loss is calculated is:

$$P_{L(Darcy)} = f \frac{L V^2 \rho}{2 ID} \quad \text{Equation 3-1}$$

Where	:	f	=	Chezy-Darcy friction factor (dimensionless)
		L	=	Length of duct (pipe) (m)
		ID	=	Internal diameter (m)
		V	=	Velocity of fluid in duct (pipe) (m/s)
		ρ	=	Density of fluid (kg/m ³)
		$P_{L(Darcy)}$	=	Pressure drop experienced over length of duct (calculated using the Darcy-Weisbach formula) (Pa)

This formula, however, requires the value for f in order to be used. The resistance that fluids encounter when flowing through pipes is dependent on whether the fluid flows through a smooth-walled pipe or a rough-walled pipe. The formula for a smooth-walled pipe was derived by Prandtl in 1953. This formula is dependent on whether the flow in the pipe is laminar or turbulent and it was thus required that the Reynolds number be calculated before the overall Chezy-Darcy friction factor number could be calculated. The formula was complemented by the equation for rough-walled pipes. These data were collated by Colebrook (in White, 1986), who developed an interpolation formula which incorporated both smooth-walled and rough-walled pipes. This formula is as follows:

$$\frac{1}{f^{1/2}} = 2.0 \times \log \left(\frac{\varepsilon/D}{3.7} + \frac{2.51}{Re_d f^{1/2}} \right) \quad \text{Equation 3-2}$$

and

$$Re_d = \frac{V d}{\nu} = \frac{V D \rho}{\mu} \quad \text{Equation 3-3}$$

Where	:	f	=	Chezy-Darcy friction factor (dimensionless)
		Re_d	=	Reynolds number
		D	=	Diameter (m)
		ϵ	=	Surface asperities (m)
		μ	=	Coefficient of viscosity (kg/ms)
		ν	=	Kinematic viscosity (m ² /s)
		ρ	=	Density (kg/m ³)

This equation was plotted by Moody into what is now referred to as the Moody Chart for pipe friction. This chart is accurate to $\pm 15\%$ for design calculations. The equation above is cumbersome to use, requiring as it does the interpolation of f until the equation balances. An alternative explicit equation was completed by Haaland. This is accurate to 2% across the range shown in the Moody chart and is (White, 1986):

$$f \approx \left\{ \frac{1}{\left(-1.8 \log \left[\frac{6.9 \mu}{\rho V ID} + \left(\frac{\epsilon / ID}{3.7} \right)^{1.11} \right] \right)} \right\}^2$$

Equation 3-4

Where	:	f	=	Chezy-Darcy friction factor (dimensionless)
		μ	=	Coefficient of viscosity (kg/ms)
		ρ	=	Density (kg/m ³)
		V	=	Velocity (m/s) (Free Air Velocity in Shafts)
		ID	=	Internal diameter (of shaft) (m)
		ϵ	=	Surface asperities (m)

It should be noted here that some texts use a value of f that is four times that defined by others. Care must therefore be taken to ensure that the correct values are used.

3.2.1.2 Atkinson calculations

The Atkinson calculation (Chasteau, 1989) was formulated for fully developed turbulent flow in an airway and is therefore applicable to flows whose Reynolds numbers exceed 4 000 ($Re > 4\ 000$). This is

usually the case for airflow in ventilation ducts. The Atkinson equation is:

$$P_{L(Atkins)} = \Delta P = \frac{k \text{ Per } L V^2}{A} \frac{\rho}{\rho_{Std}} \quad \text{Equation 3-5}$$

Where	:	k	=	Atkinson friction factor (NS^2/m^4)
		L	=	Length of airway (m)
		Per	=	Perimeter of airway (m)
		A	=	Cross-sectional area of airway (m^2)
		V	=	Velocity of fluid in airway (m/s)
		ρ	=	Density of fluid (kg/m^3)
		ρ_{Std}	=	Standard density of fluid (kg/m^3) (usually $1.2 kg/m^3$)
		$P_{L(Atkinson)}$	=	Pressure drop experienced over length of duct (calculated using Atkinson equation)(Pa)

An additional parameter that can be defined from this equation is that of airway resistance (R). The equation for this is:

$$R = \frac{k \text{ Per } L}{A^3} \frac{\rho}{\rho_{Std}} \quad \text{Equation 3-6}$$

Where	:	k	=	Atkinson friction factor (NS^2/m^4)
		L	=	Length of airway (m)
		Per	=	Perimeter of airway (m)
		A	=	Cross-sectional area of airway (m^2)
		ρ	=	Density of fluid (kg/m^3)
		ρ_{Std}	=	Standard density of fluid (kg/m^3) (usually $1.2 kg/m^3$)
		R	=	Airway resistance due to wall roughness (Ns^2/m^8)

The values of k (the Atkinson friction factor) are taken from tables of measurements which have been compiled in the past. These values are readily available from any mine ventilation text.

This form of the calculation has the advantage of being widely used in mine ventilation circles. However, it has two shortcomings:

- 1 The values of k are measured at different fluid densities and therefore the data must

always be correct for the current circumstances before they can be used. This also implies that the data are not geometrical measures of airway resistance as they depend on this air density.

and

- 2 The exact circumstances surrounding the measurement of the data points is not known and inaccuracies can therefore develop if there are significant differences.

3.2.1.3 Rational resistance

The definition of the rational resistance as defined by McPherson (1971) is shown in the equation below:

$$f = 2 \frac{k}{\rho_{Std}} \quad \text{Equation 3-7}$$

and

$$\Gamma = \frac{R}{\rho} \quad \text{Equation 3-8}$$

Where	:	k	=	Atkinson friction factor (Ns ² /m ⁴)
		f	=	Chezy-Darcy friction factor
		ρ	=	Density of fluid (kg/m ³)
		ρ _{Std}	=	Standard density of fluid (kg/m ³) (usually 1.2 kg/m ³)
		R	=	Airway resistance due to wall roughness (Ns ² /m ⁸)
		Γ	=	Rational resistance (m ⁻⁴)

Γ is termed the 'rational resistance' and depends only on the airway geometry and roughness; it is independent of air density. The relationship between Γ and the Chezy-Darcy friction factor *f* is defined in the following equation:

$$\Gamma = \frac{f}{2} \times \frac{Per \times L}{A^3} \quad \text{Equation 3-9}$$

Where	:	f	=	Chezy-Darcy friction factor (dimensionless)
		L	=	Length of airway (m)
		Per	=	Perimeter of airway (m)
		A	=	Cross-sectional area of airway (m ²)

$$\Gamma = \text{Rational resistance (m}^{-4}\text{)}$$

The pressure loss is calculated from the following equation:

$$P_{L(\text{Rational})} = \Gamma \rho (V A)^2 = \Gamma \rho Q^2 \quad \text{Equation 3-10}$$

Where	:	Γ	=	Rational resistance (m ⁻⁴)
		L	=	Length of airway (m)
		V	=	Velocity of fluid in airway (m/s)
		A	=	Cross-sectional area of airway (m ²)
		ρ	=	Density of fluid (kg/m ³)

3.2.2 Shaft Friction Resistance

The current theory for the calculation of this resistance assumes that the resistance values each of the resistance sources listed below is independent of the others. This assumption is not strictly true but is required for the calculation to be completed.

The shaft friction resistance is calculated with respect to three criteria:

- i Friction resistance (standard fluid theory based on the Moody chart)
- ii Resistance offered by the shaft fittings (buntons, guides, pipes, etc.)
- iii Resistance offered by the movement of the conveyances in the shaft

Thus the overall Chezy-Darcy friction factor for the shafts is calculated by summing the individual Chezy-Darcy friction factors for each of the resistant components in the shaft

$$f_{\text{Total}} = f_{\text{Shaft}} + f_{\text{Buntons}} + f_{\text{Guides}} + f_{\text{Fittings}} + f_{\text{Cages}} \quad \text{Equation 3-11}$$

Where	:	f_{Total}	=	Combined Chezy-Darcy friction factor of complete shaft (dimensionless)
		f_{Shaft}	=	Chezy-Darcy friction factor for shaft wall (dimensionless)
		f_{Buntons}	=	Chezy-Darcy friction factor for shaft buntons (dimensionless)
		f_{Guides}	=	Chezy-Darcy friction factor for shaft guides (dimensionless)
		f_{Fittings}	=	Chezy-Darcy friction factor for shaft fittings (dimensionless)
		f_{Cages}	=	Chezy-Darcy friction factor for cages (dimensionless)

3.2.2.1 Friction resistance of shaft

The resistance that the shaft offers to ventilation airflow is calculated in accordance with the theory laid out in Section 3.2.1.1.

3.2.2.2 Resistance offered by shaft fittings

Longitudinal fittings

These fitting include pipes, guides, cables and other fittings which run parallel to the airflow through the shaft. According to both Bromilov and McPherson, model shaft tests have shown that these fittings can actually reduce the overall Chezy-Darcy friction factor of the shaft. Nevertheless, allowance is made for the longitudinal fittings by decreasing the effective shaft cross-sectional area by the cross-sectional area of these fittings.

The reduced 'effective' shaft diameter is then used for further calculation of the overall shaft losses.

Buntons

Buntons differ significantly from longitudinal fittings in that longitudinal fittings offer resistance to the airflow via boundary layer friction, whereas buntons form obstructions to the airflow perpendicular to that flow.

To calculate the overall pressure drop in the shaft it is also necessary to derive a Chezy-Darcy friction factor for the shaft fittings. To calculate the friction offered by the buntons, the aerodynamic drag of the buntons is considered. This is used to calculate the friction resistance of each of the buntons. This resistance is then multiplied by the number of buntons in the shaft and an overall buntion Chezy-Darcy friction factor for the shaft is calculated as follows:

$$f_{\text{Buntions}} = \frac{C_d A_b}{S \text{ Per}} \quad \text{Equation 3-12}$$

Where :

- C_d = Drag coefficient (dimensionless)
- A_b = Frontal area of buntions (facing airflow) (m^2)
- S = Spacing between buntions (m)
- Per = Perimeter of shaft (m)

and

$$\Gamma_{\text{Buntions}} = \frac{L}{S} C_d \frac{A_b}{2A_{FS}^3}$$

Equation 3-13

Where	:	Γ_{Buntions}	=	Rational resistance of buntions (m^{-4})
		L	=	Length of shaft (m)
		C_d	=	Drag coefficient (dimensionless)
		A_b	=	Frontal area of buntions (facing airflow) (m^2)
		S	=	Spacing between buntions (m)
		A_{FS}	=	Free cross-sectional area of shaft for flow (m^2)

However, the above assumes that the frictional resistance of each of the buntions is independent of that of the following buntion. This means that it is assumed that the turbulent eddies for each buntion set die out before the flow reaches the next buntion set. In reality, this is unlikely to happen. To mitigate against this Bromilov evaluated a total of 24 shafts of varying roughnesses and fitting regimes. This evaluation results in an interference factor (F) being introduced, which has the effect of reducing the overall resistance of the shaft and bringing it more in line with the modelled tests.

$$F = 0.0035 \frac{S}{W} + 0.44$$

Equation 3-14

Where	:	F	=	Interference factor (dimensionless)
		S	=	Buntion spacing (m)
		w	=	Width of buntions (m)

To obtain the appropriate frictional resistance of the buntions for inclusion in the Darcy-Weisbach calculation, the following formula is used:

$$f_{\text{Bu}} = C_D \times \frac{A_b}{S \times \text{Per}} \left(0.0035 \times \frac{S}{W} + 0.44 \right)$$

Equation 3-15

Where	:	C_D	=	Coefficient of drag for buntions
		A_b	=	Frontal area of buntions (m^2)
		S	=	Spacing between buntions (m)
		Per	=	Perimeter of shaft (m)
		W	=	Width of buntions (m)

and

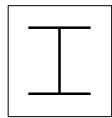
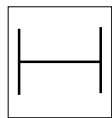
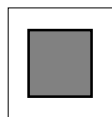
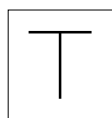
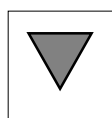
$$\Gamma_{Bu} = \frac{L}{S} \times C_D \times \frac{A_b}{2 \times A_{FS}^3} \left(0.0035 \times \frac{S}{W} + 0.44 \right) \quad \text{Equation 3-16}$$

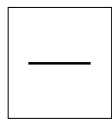
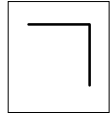
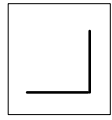
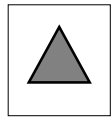
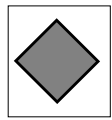
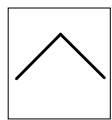
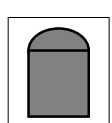
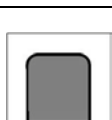
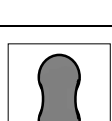
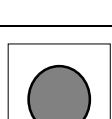
- Where :
- C_D = Coefficient of drag for buntions
 - Γ_{Bu} = Rational resistance of buntions (m^{-4})
 - A_b = Frontal area of buntions (m^2)
 - A_{FS} = Free cross-sectional area of shaft (m^2)
 - S = Spacing between buntions (m)
 - W = Width of buntions (m)

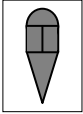
The results of these calculations then used to calculate the overall frictional resistance of the shaft in accordance with the three calculations discussed above.

In the interests of clarity, Table 3-1 contains the coefficients of drag for the various buntion shapes.

Table 3-1: Summary of drag coefficients of elongated bodies of infinite span (McPherson, 1987)

1		I - Girder	2.75	Skonchinsky (1952)
2		I – Girder	2.05	Hoerner (1951)
3		Rectangle	2.05	Hoerner (1951)
4		Tee	2.00	Hoerner (1951)
5		Triangle	2.00	Hoerner (1951)

6		Plate	1.98	Hoerner (1951)
7		Angle	1.98	Hoerner (1951)
8		Angle	1.82	Hoerner (1951)
9		Triangle	1.55	Hoerner (1951)
10		Square	1.55	Hoerner (1951)
11		Angle	1.45	Hoerner (1951)
12		Capped Rectangle	1.40	Estimated from results by Skonchinsky (1951) and Bareza and Hounerchts (1955)
13		Rounded Square	1.35	Approximate value – value depends on the ratio: radius of corner side of square
14		Dumbbell	1.30	Calculated from Martinson's results (1957)
15		Cylinder	1.20	Hoerner (1951)

16		Streamlined girder	1.03	Skonchinsky (1952)`
----	---	--------------------	------	---------------------

3.2.2.3 Resistance offered by shaft cages

The resistance that the cage, skip or counterweight offers to the flow of air through the shaft is considered in two steps, namely:

- 1 The resistance as a result of the obstruction that the cage, skip or counterweight offers to the flow of air in the shaft
- 2 The transient effects which cause resistance to the airflow as a result of the motion of the conveyance in the shaft

Resistance due to obstruction

The standard equation for the 'shock' or pressure loss incurred by the flow of air when it is caused to change direction by an obstruction is as follows:

$$P_{SC} = X \rho \frac{V^2}{2} \tag{Equation 3-17}$$

- Where :
- P_{SC} = Pressure loss from stationary cage (Pa)
 - X = Shock loss factor
 - ρ = Density of airstream (kg/m^3)
 - V = Velocity of approaching airstream (m/s)

and

$$P_{SC} = \rho \Gamma_{conv} V^2 A_{FS}^2 \tag{Equation 3-18}$$

- Where :
- P_{SC} = Pressure loss from stationary cage (Pa)
 - Γ_{conv} = Rational resistance of conveyance (m^{-4})
 - ρ = Density of airstream (kg/m^3)
 - V = Velocity of approaching airstream (m/s)
 - A_{FS} = Area of free shaft section (m^2)

and

$$\Gamma_{\text{Conv}} = \frac{X}{2 A_{\text{FS}}^2} \quad \text{Equation 3-19}$$

Where :

- Γ_{Conv} = Rational resistance of conveyance (m^{-4})
- X = Shock loss factor
- A_{FS} = Free cross-sectional area of shaft (m^2)

The evaluation of X must now be completed. A comprehensive study of cage resistances was carried out by Stevenson (1956). McPherson (1987) performed the most recent analysis of these data. The results of this analysis are presented in Figure 3-1. These data show the variation of X with respect to the coefficient of fill (C_f) of the conveyance in the shaft.

$$C_f = \frac{A_{\text{Conv}}}{A_{\text{FS}}} \quad \text{Equation 3-20}$$

Where :

- C_f = Coefficient of fill
- A_{FS} = Free cross-sectional area of shaft (m^2)
- A_{Conv} = Frontal cross-sectional area of the conveyance (m^2)

The data in Figure 3-1 refer specifically to the length over width ratio of 1.5 and apply to a range of conveyances with height over width ratios of 1.5–6.0. These data can be extrapolated to suit all cages by multiplying the result by the correction factor which corresponds to the length over width ratio considered in any specific analysis.

In addition, the tests were completed on conveyances with open ends. In the case of cages or skips with closed ends, the X factor should be reduced by approximately 15% (Bromilov, 1960).

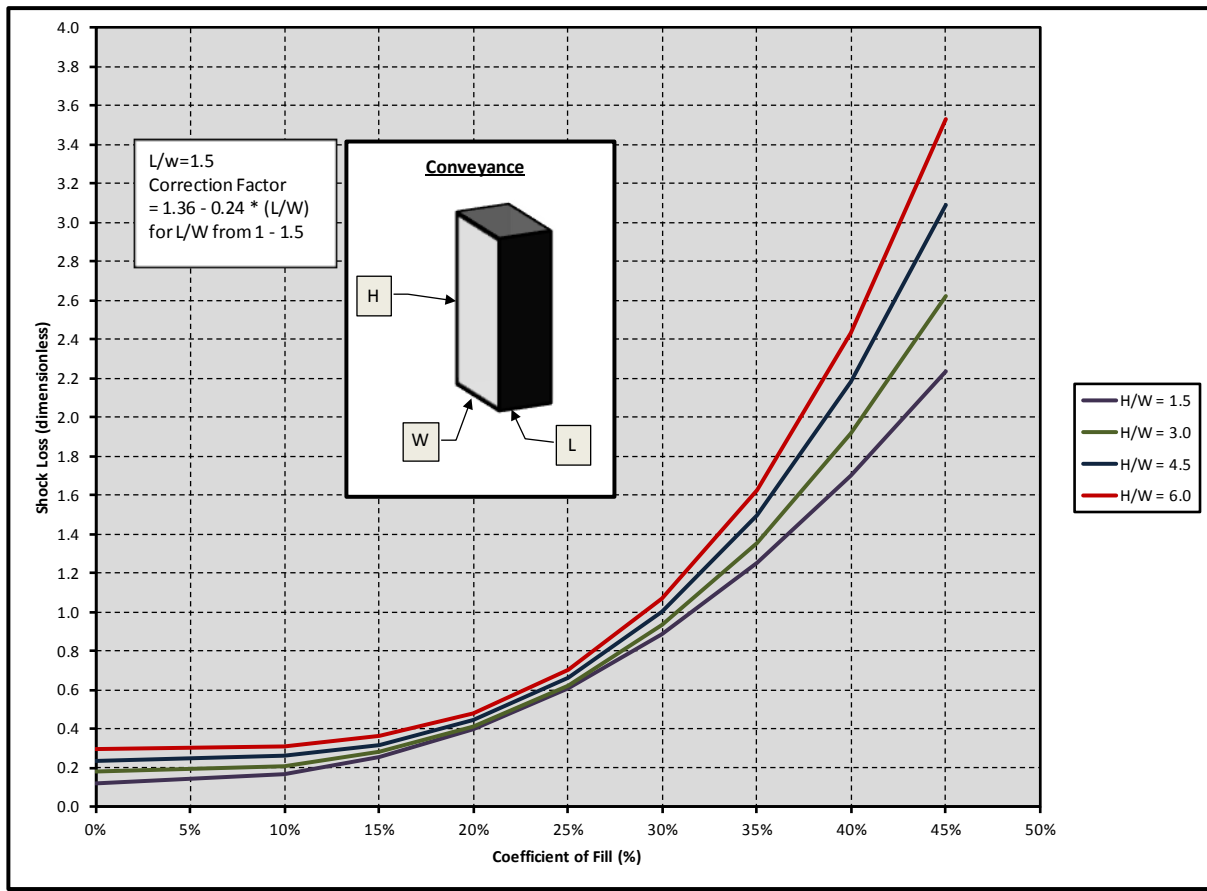


Figure 3-1: Conveyance shock loss estimation for conveyances

Resistance due to cage movement

The standard equation for pressure loss over an obstruction was defined in Equations 3–1 to 3-7. In order to calculate the maximum pressure loss for a cage that is moving, a slight modification is required to this equation. The equation is defined by the expression for an obstruction blocking airflow in a shaft and it is also assumed that the cage is standing still and that the velocity of the flow of air around the cage is equal to the velocity of the cage itself (V_{Conv}).

$$P_{MC} = X \rho \frac{V_{Conv}^2}{2} \tag{Equation 3-21}$$

- Where :
- P_{MC} = Pressure loss from moving cage (Pa)
 - X = Shock loss factor
 - ρ = Density of airstream (kg/m^3)
 - V_{Conv} = Velocity of conveyance (m/s)

There are two possible exist when calculating the pressure loss over a moving conveyance, namely:

- i The conveyance is moving in the same direction as the airflow. (The two expressions are added.)
- ii The conveyance is moving in the opposite direction to the airflow. (The two expressions are subtracted.)

$$P_{MC(Max)} = P_{SC} \left(1 + \frac{V_{Conv}^2}{V_{FS}^2} \right) \quad \text{Equation 3-22}$$

and

$$P_{MC(Min)} = P_{SC} \left(1 - \frac{V_{Conv}^2}{V_{FS}^2} \right) \quad \text{Equation 3-23}$$

- Where :
- $P_{MC(Max)}$ = Maximum pressure loss from moving cage (Pa)
 - $P_{MC(Min)}$ = Minimum pressure loss from moving cage (Pa)
 - V_{FS} = Free shaft velocity of approaching airstream (m/s)
 - V_{Conv} = Velocity of conveyance (m/s)
 - P_{SC} = Pressure loss from stationary cage (Pa)

The effective resistance of a moving conveyance can also be determined from the following:

$$P_{MC(Max)} = \Gamma_{MC(Max)} \rho V_{FS}^2 A_{FS}^2 \quad \text{Equation 3-24}$$

and

$$P_{MC(Min)} = \Gamma_{MC(Min)} \rho V_{FS}^2 A_{FS}^2 \quad \text{Equation 3-25}$$

- Where :
- $P_{MC(Max)}$ = Maximum pressure loss from moving cage (Pa)
 - $P_{MC(Min)}$ = Minimum pressure loss from moving cage (Pa)
 - V_{FS} = Free shaft velocity of approaching airstream (m/s)
 - $\Gamma_{MC(Max)}$ = Maximum rational resistance of moving conveyance (m^{-4})
 - $\Gamma_{MC(Min)}$ = Minimum rational resistance of moving conveyance (m^{-4})
 - ρ = Density of airstream (kg/m^3)
 - A_{FS} = Free cross-sectional area of shaft (m^2)

The rational resistance is defined as:

$$\Gamma_{MC(Max)} = \Gamma_{Conv} \left(1 + \frac{V_{Conv}^2}{V_{FS}^2} \right) \quad \text{Equation 3-26}$$

and

$$\Gamma_{MC(Min)} = \Gamma_{Conv} \left(1 - \frac{V_{Conv}^2}{V_{FS}^2} \right) \quad \text{Equation 3-27}$$

Where	:	V_{FS}	=	Free shaft velocity of approaching airstream (m/s)
		V_{Conv}	=	Velocity of conveyance (m/s)
		$\Gamma_{MC(Max)}$	=	Maximum rational resistance of moving conveyance (m ⁻⁴)
		$\Gamma_{MC(Min)}$	=	Minimum rational resistance of moving conveyance (m ⁻⁴)
		Γ_{Conv}	=	Rational resistance of conveyance (m ⁻⁴)

3.2.3 Accuracy Limits of the Theory

All the calculations described above are based on empirical values to which formulas are fitted in order to calculate the overall resistance of a shaft. Each of the particular areas discussed will now be evaluated in turn.

3.2.3.1 Accuracy of calculation for friction resistance of shaft

As was noted above, this calculation is based on the theory for flow of fluids through ducts. The Moody chart used for determination of the frictional resistance has an overall accuracy of $\pm 15\%$ for design calculations. In addition, the simplifying formula developed has an accuracy of $\pm 2\%$ across the range. This means an overall accuracy of 17.6%. This is directly proportional to the calculation and must be considered when the overall accuracy of the results is calculated.

However, the resistance offered by the shaft walls generally accounts for between 10% and 15% of the overall resistance of the shaft. This results in a potential inaccuracy of 0.2% for the shaft resistance calculation.

3.2.3.2 Accuracy of calculation for resistance offered by shaft fittings

The resistance offered by the shaft fittings is generally more than 80% of the overall shaft resistance. The accuracy of these calculations therefore makes the most significant contribution to the overall

accuracy. Paradoxically, the accuracy of these calculations is also the most difficult to quantify.

This evaluation consists initially of the values used for the drag coefficients of the buntons and the associated simplifying assumptions (discussed above). These values cannot be evaluated in isolation. Bromilov (1960) introduced an interference factor (F) to account for the effect the buntons will have on each other in relation to the flow of air through the shaft.

These results showed that for smooth-walled shafts, the drag coefficient and interference factor resulted in accuracies of $\pm 15\%$ against the measured values. This accuracy deteriorated abruptly when used for rough-walled shafts. This shows that the calculation must be used with care to ensure its validity for various shafts. No attempt was made to quantify the accuracy of the calculation with additional inclusions such as ladderways.

3.2.3.3 Accuracy of calculation for resistance offered by shaft cages

All the theory available for evaluation of the conveyances in a shaft is based on the work done by Stevenson (1956). In this work he used a horizontal duct of circular cross-section, 0.286 m (11¼ inches) in diameter and 27.432 m (90 ft) long. The tests were carried out over a range of Reynolds numbers. These data were analysed and re-used by McPherson (1987). They have not been verified and the accuracy of the calculations based on these measurements is therefore not known.

3.2.3.4 General comments on the accuracy of the theory

In CHAPTER 2 numerous papers were evaluated in order to try and obtain a clearer understanding of the actual accuracy of the current theory. The only paper that was found specifically to test the accuracy of these calculations was that by Deen (1991). In this paper he noted the accuracy of the theoretical calculation to be less than 5% on three of the shafts and 11.8% on the final shaft. Unfortunately, no information was supplied on how the tests were done or on the assumptions used for the basis of the calculation. Neither was a detailed comparison of the results given.

3.3 VALIDATION OF EXISTING THEORY AND INITIAL SHAFT TESTS

The necessary equations for calculating the theoretical pressure drop for the shaft have been provided in Section 3.2. As was noted in CHAPTER 2 of this document, few data are available to confirm the efficacy of these equations. In this regard Impala Platinum Mines was approached and the management kindly agreed to allow tests to be conducted on No. 14 shaft. The only proviso they attached to this was that the tests should not interrupt production in any manner or form.

3.3.1 Test Methodology

The details of the test methods available are discussed in Section 2.2.4 and will not be repeated here. In the tests conducted for this work, the density method of measurement was used. The reason for this is twofold:

- 1 The accuracy of the barometer has improved significantly and it can be used with ease.
- 2 As the tests were run on a continuous basis, no inclusions in the shaft were allowed.

This method consists of the simultaneous measurement of the following parameters (Hemp, 1989):

- 1 Barometric pressures (at point 1 and point 2)
- 2 Airflow
- 3 Wet-bulb temperature
- 4 Dry-bulb temperature

In addition, the two elevations should be known.

Once these parameters are known, the pressure loss can be calculated using the following equations:

$$P_{L(\text{meas})\text{oss}} = - (P_2 - P_1) - g \times \int w \, dZ \quad \text{Equation 3-28}$$

Where	:	$P_{L(\text{meas})}$	=	Measured pressure loss (Pa)
		P_1	=	Barometric pressure at point 1 (Pa)
		P_2	=	Barometric pressure at point 2 (Pa)
		g	=	Gravitational constant (m/s^2)
		$\int w dZ$	=	Theoretical pressure increase (Pa)

and

$$\int w \, dZ = 0.5 \times (\rho_1 + \rho_2) \times (Z_2 - Z_1) \quad \text{Equation 3-29}$$

Where	:	ρ_1	=	Calculated density at point 1 (kg/m^3)
		ρ_2	=	Calculated density at point 2 (kg/m^3)
		Z_1	=	Elevation at point 1 (m)
		Z_2	=	Elevation at point 2 (m)

3.4 TESTS USED TO VALIDATE THEORY

3.4.1 Test Methodology

For calculation of the pressure loss in a shaft as a result of its fittings, the ideal testing parameters would be as follows:

- 1 The shaft ventilation will remain constant.
- 2 The instruments used to measure the pressure, temperature and velocity must be placed in the shaft such that their placement will not interrupt the normal ventilation flow.
- 3 These instruments must be allowed to remain in place for a sufficient length of time to allow any movement in the measurements to subside.

During this test period the shaft must not be used for anything else. These requirements are, however, not possible to achieve as they would interrupt the production of the shaft.

It was therefore decided to complete the initial testing during the weekly shaft examinations. This had the advantage that the movement of the cages would be predictable and would also be at a slow speed; thus they would not affect the pressure readings significantly.

3.4.1.1 Main downcast shaft test procedure

Velocity

The main cage was chosen as the platform from which to take the necessary readings. One of the chief concerns was the measurement of the shaft ventilation velocity in an area where the measurement platform would not affect the readings. This concern was dealt with by using a Pitot tube arrangement. The Pitot itself was attached to a bracket which was in turn attached to the rope of the conveyance. This kept the tube at right angles to the ventilation air and also well above the cage. Thus the bulk of the cage did not affect the readings taken from it. The trailing tubes were lowered into the cage where the readings could be taken without hindrance.

Shaft inspections are normally done with all the conveyances moving down the shaft within shouting distance of each other. This would also have created a blockage and have affected the ventilation airflow. As a result, when the cage was stopped to take the measurement, the other conveyances were asked to move slightly further down the shaft.

Pressure

The pressure measurements were taken using a standard barometer. One of the concerns here was the spacing at which the measurements would be taken. In order to ensure these spacings were the

same, readings were taken every 20 bunton sets.

Temperatures

Wet and dry-bulb temperatures were taken using a standard whirling hygrometer. These were taken outside the cage to ensure that no insulating effect was apparent from within the cage.

Testing

In order to do the tests, it was requested that the cage be stopped at regular intervals while moving down the shaft. These intervals were counted and the cage was stopped to allow measurements to be taken every 20 bunton sets. At each point the following measurements were taken:

- 1 Wet-bulb temperature (T_{WB}) (°C)
- 2 Dry-bulb temperature (T_{DB}) (°C)
- 3 Velocity pressure (P_v) (Pa)
- 4 Static pressure (P_{Static})
- 5 Total pressure (P_{Tot})
- 6 Barometric pressure (P_{Bar})

Once the uninterrupted portion of the shaft had been tested, additional tests were done from just above each of the stations.

3.4.1.2 Test procedure in the rest of the mine shafts

The No. 14 shaft complex has a total of four shafts – two downcast and two upcast shafts. These are shown in Figure 1-9.

Each of these was tested in turn. The detailed results are presented in Appendix D. It was not possible to take measurements over the length of the upcast shaft or the length of the unequipped downcast shaft. In addition, although it was possible to measure the velocity and pressure in the upcast shaft from the fans, it was not possible to do this in the downcast shaft. However, the bulk air cooler and refrigeration systems were not in operation as it was winter, so it was possible to obtain general barometric and temperature readings from the shaft head. Figure 3-2 and Figure 3-3 show the brackets that were used to attach the Pitot tube to the conveyance rope, as well as the instrumentation used for this test. Figure 3-4 shows the remainder of the instrumentation used.

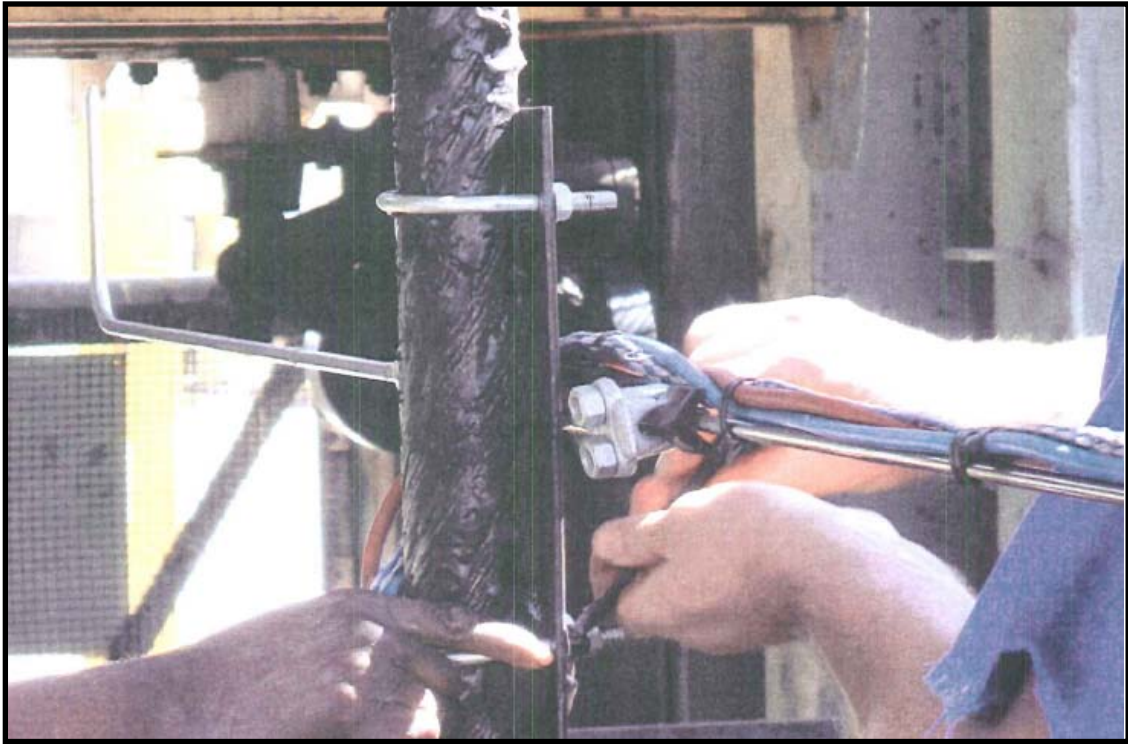


Figure 3-2: Pitot tube attachment bracket on rope above cage



Figure 3-3: Pitot tube attachment bracket (above cage)



Figure 3-4: Testing instrumentation – Pitot tube, barometer and whirling hygrometer

3.4.1.3 Accuracy and repeatability of test data

The following instruments were used for this evaluation:

- 1 ALNOR AXD – Pitot measurement
- 2 GPB 2300 – Barometric measurement
- 3 Whirling hygrometer

ALNOR AXD

Pressure	-	Range	:	-3 700–3 700 Pa
		Accuracy	:	±1% of reading
		Resolution	:	1 Pa
Velocity	-	Range	:	1.27–78.70 m/s
		Accuracy	:	±1.5% of reading

	Resolution	:	0.1 m/s
Operating temperature		:	5– 45°C

GPB 2300

Range	:	0–130 kPa
Accuracy	:	±0.25% of reading
Resolution	:	100 Pa
Operating temperature	:	-25–50°C

Whirling hygrometer

Range	:	0–50 °C
Accuracy	:	±2% of reading
Resolution	:	0.5 °C
Operating temperature	:	0–50°C

These accuracies are considered to be acceptable and should result in a cumulative accuracy of less than 5%.

3.4.1.4 Ideal test methodology

As was noted in the previous section, the indirect testing method is not ideal given the constraints of the accuracy requirements noted. In this regard, once the overall testing had been completed, the accuracy of these measurements was evaluated in line with the recommended procedures described above. The tests showed accuracies of 0.3%, thus indicating that the concerns raised were dealt with successfully in the methodology.

This is due primarily to the static nature of the tests (i.e. the conveyance was brought to a halt), as well as to the removal of dynamics in the shafts during the tests. The tests were therefore deemed to be acceptable.

3.4.2 Results of Tests

The detailed calculation of the test results can be found in Appendix D. However, a summary of the results is given in Table 3-2.

Table 3-2: Impala No. 14 shaft – details of tested shafts

No. 14 shaft	No. 14 V shaft	No. 14 A shaft	No. 14 B shaft	Units	Symbol	Description
7.4	4.9	5.6	5.8	m	diam.	Diameter of shaft
23.2	15.4	17.6	18.2	m	per	Perimeter of shaft
38.0	18.8	24.6	26.4	m ²	A _{FS}	Free cross-sectional area of shaft
868	620	1 060	1 152.6	m	L _{S (AS)}	Length of shaft (stops above the airway split)
10.1	17.2	21.1	15.6	m/s	V _{Shaft Average}	Average velocity of air in shaft (Free Air Velocity)
384	323	520	411	m ³ /s	Q	Volumetric flow rate in shaft
1.14	1.03	1.097	1.18	kg/m ³	ρ _{Average in Shaft}	Average density in shaft
437	334	570	484	kg/s	G	Volumetric flow rate in shaft
0.017	0.009	0.002	0.005	Ns ² /m ⁴	k	Measured Atkinson friction factor
0.014	0.006	0.003	0.006	Ns ² /m ⁴	k	Calculated Atkinson friction factor (Darcy-Weisbach)
0.021	0.003	0.004	0.003	Ns ² /m ⁴	k	Calculated Atkinson friction factor (rational resistance)
Measured Atkinson friction factor				This Atkinson friction factor was calculated based on the measured pressure losses.		
Calculated Atkinson friction factor (Darcy-Weisbach)				This Atkinson friction was calculated using McPherson's methodology using the Darcy-Weisbach option.		
Calculated Atkinson friction factor (rational resistance)				This Atkinson friction was calculated using McPherson's methodology using the Rational Resistance option.		
The shaft has standard concrete lining.						
Data from <i>Environmental Engineering in SA Mines</i> (Lloyd, 1989):						

Atkinson friction factor (Ns^2/m^4)			Description
0.0040	-	-	Concrete lined – No steelwork
0.0045	-	0.0250	Concrete lined – streamlined buntions
0.0075	-	0.0600	Concrete lined – RSJ buntions
0.0450	-	0.0900	Timbered rectangular shafts

As can be concluded from the data in Table 3-2, there is reasonable correlation between the data calculated and the data measured. This is in spite of the differences between the shafts. Three of these shafts were unequipped ventilation shafts (both upcast and downcast). The shaft of particular interest is No. 14 shaft as this is a fully equipped downcast shaft with a full suite of conveyances. The difference between the fan pressure and the flow rate can be found in tabular form in Table 1-2 and the mine configuration in Figure 1-8.

3.4.3 Conclusion and Recommendations

This shaft is equipped with streamlined buntions and is generously spaced with respect to the free area available for airflow. The Chezy-Darcy friction factors, both measured and calculated, were within the expected range. The rational resistance value calculated was, however, significantly higher than those of the measured value and the Chezy-Darcy friction factor value. This is attributed to the inaccuracies from the estimations in the calculation. These inaccuracies are detailed in Section 2.2.

These data show good correlation between the theory and the practice. It is thus appropriate to move on to the next phase of testing and that is to measure the pressure losses resulting from the dynamic nature of the moving conveyances.

3.4.4 Innovative Testing Methodology

To measure the pressure losses in a shaft, an innovative testing methodology is required which will allow remote testing of the shaft. This is primarily born out of the need to be able to measure various parameters in the shaft during normal operation. The following parameters are required:

- 1 Dry-bulb temperature (T_{DB}) ($^{\circ}C$)
- 2 Wet-bulb temperature (T_{WB}) ($^{\circ}C$) (or relative humidity, %)
- 3 Velocity of air in shaft (m/s)

- 4 Barometric pressure (P_{Bar})
- 5 Position and speed of all the conveyances in the shaft

All these measurements will be needed as functions in time so that meaningful calculations can be made with respect to actual pressure losses and the overall effect of the movement of the conveyances.

Ideally, the instrumentation should be placed in position and the various conveyances should then be allowed to move individually in the shaft so that the specific parameters for each of these can be measured and the pressure losses calculated. The data from the individual instruments would then be collated on a single computer to enable real-time comparisons to be made.

Unfortunately, this is not achievable as a result of the shaft time that would be required. Moreover, the necessary instrumentation and data-transfer mechanisms are expensive and difficult to install. Although most shafts already have data-transfer systems, these are used for production and, as stated earlier, the one proviso that Impala Platinum stipulated for these tests was that no interruption of production was to take place.

For this reason logging instrumentation was sought which would measure the required parameters at a set interval and log the results for later retrieval.

3.5 TESTS CONDUCTED ON SHAFTS

After discussion with the mine management, it was decided that the ideal time to put the instrumentation in place in the shaft would be during the weekly shaft inspections, for which purpose the testers would have to accompany the mine personnel on the inspection. This would have the benefit of allowing the testers to review the shaft arrangement and to take ventilation velocity measurements during the inspection.

It would not be possible to place the instrumentation in the shaft itself given the sensitivity of anything being placed in the shaft barrel and its potential effect on production. Thus the instruments would have to be placed immediately adjacent to the barrel on the stations. These instruments would then remain in place for at least a week before they could be recovered during subsequent shaft visits.

3.5.1 Equipment Used

3.5.1.1 Environmental instrumentation

The instrumentation required for the environmental tests had to have the following characteristics:

- 1 Must be able to measure the parameters at set intervals and log the data measured (a maximum interval of 10 seconds was chosen).
- 2 Must be insulated against the environment so that dust and moisture could not affect the readings.
- 3 Must have sufficient accuracy to allow the various measurements to be reliable.
- 4 Must be small and easy to transport and install.

These criteria were met by the EASYlog 80CL supplied by Greisinger. The instrument cannot measure the wet-bulb temperature, but it does measure the moisture content of the air. The EASYlog 80CL is battery operated and can withstand a harsh environment. The specifications of this instrument are listed in Table 3-3 and a photo picture of such a logger is shown in Figure 3-5.

Table 3-3: EASYlog 80CL specifications

Description	Measuring range		
Temperature	-25.0 °C	-	+60 °C
Humidity	0.0%	-	100.0%
Air pressure	30 kPa	-	110 kPa
	Resolution		
Resolution	0.1 °C	0.1% RH	0.01 kPa
	Accuracy (± 1 digit)		
Temperature	± 0.3 °C		
Humidity	± 2% RH (at range 0–90% RH)		
Air pressure	± 0.1 kPa (typical) – ±0.25 kPa (maximum)		
Nominal temperature	25 °C		
Operating temperature	-25.0 °C	-	+60 °C

Battery life			
Measuring cycle	4 seconds	3 minutes	15 minutes
Record period	11.5 days	521 days	7.1 years



Figure 3-5: EASYLog 80CL

3.5.1.2 Winder measurements

To ensure that the position of the various conveyances in the shaft is known, it is necessary that rotary encoders be connected to the winder. This did pose something of a problem as the only encoders available are digital encoders, which require logging from the PLC. The following combination was chosen.

Ruggedised rotary encoders from Leine and Linde, connected to a standard Honeywell PLC, operated using a standard touch screen interface, were chosen for this application. These encoders are attached to the shaft on the winder in question and therefore measure the overall revolutions of the winder. This arrangement requires a 220 V connection. This is considered a weakness as the early

tests showed that this connection was broken either by power trips on the shaft or personnel removing plug connections. To ensure that the status of these connections was known at all times, a GSM module was also attached to the PLC. Figure 3-6, Figure 3-7 and Figure 3-8 show the set-up.

These encoders have an operating range of -40 to 70 °C and are sufficiently accurate to measure up to 5 000 increments on a revolution. The PLC was programmed to store data every second and to record 50 points on each rotation. This is sufficient to allow the calculation of the position of each conveyance, as well as to calculate acceleration and deceleration.

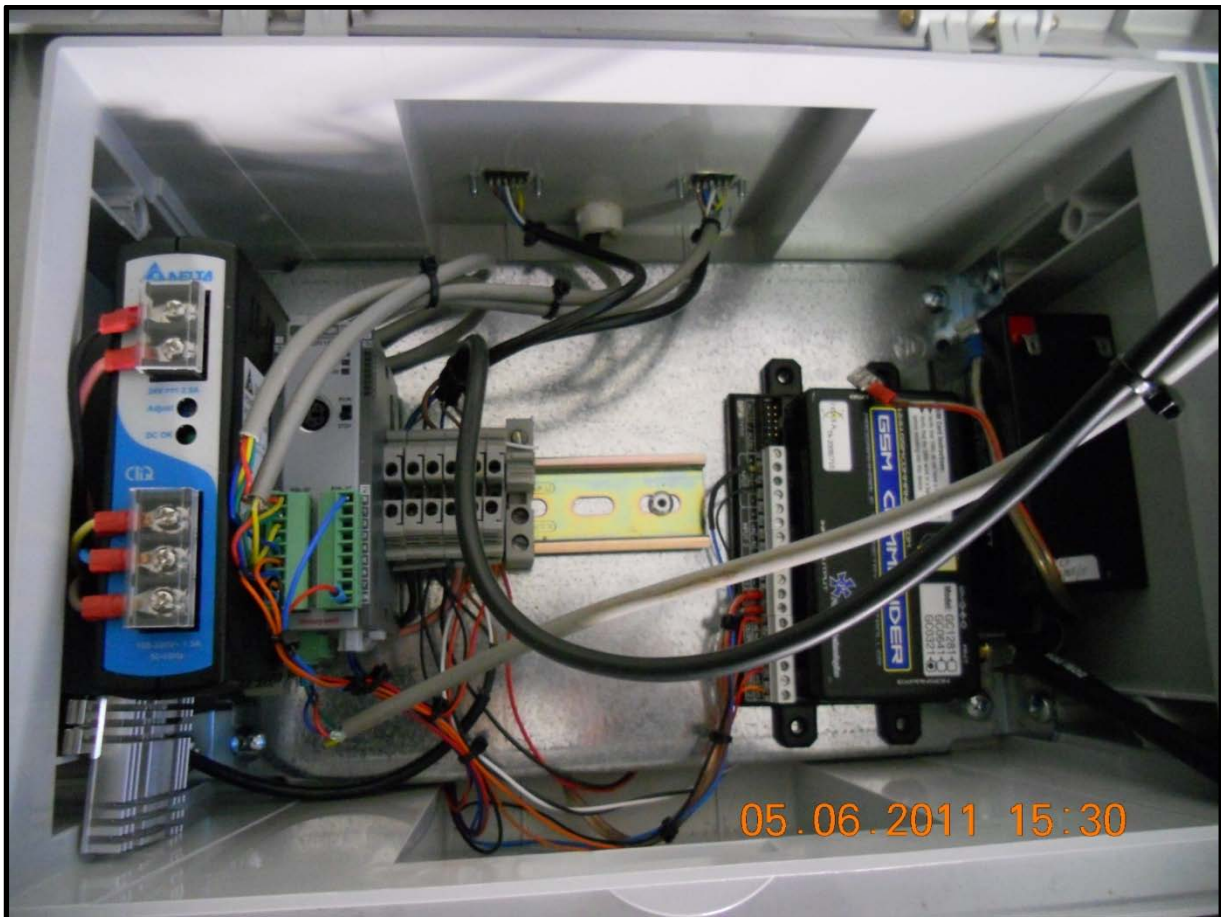


Figure 3-6: PLC, interface and GSM module for rotary encoder



Figure 3-7: Rotary encoder



Figure 3-8: Rotary encoder connection on winder side shaft

3.5.1.3 Velocity measurements

The velocity measurements were taken during the shaft tests using a hand-held anemometer. These results were then compared with the information available from the ventilation department to ensure accuracy and consistency.

The instrument used was a Kestrel 4000 (see Figure 3-9), with the following specifications:

Range	:	0.4–60 m/s
Accuracy	:	±3% of reading
Resolution	:	0.1 m/s
Operating temperature	:	-29–70°C



Figure 3-9: Kestrel 4000 environmental logger

3.5.2 Data Collection and Collation

3.5.2.1 Data collection

The general procedure for the collection of data involved firstly the preparation of the instrumentation. This required confirmation of the battery life of the instrumentation, clearing of the logged data and synchronisation of all the instrumentation to a single computer. This was a specific

requirement because the various loggers were not connected and the single reference time point was therefore the only point that would allow the various measurements to be compared.

The environmental loggers were placed in positions that were determined in consultation with the mine ventilation officer. They were placed during the shaft inspection. During this inspection the shaft ventilation free air velocity was confirmed and the general condition and layout of the shaft was evaluated.

Once this had been completed, the loggers for the winders were put in place and the logging started.

All the instruments logged data for one week, at the end of which they were removed during the next scheduled shaft inspection.

3.5.2.2 Data collation

Once the data from the various loggers had been collected, they were all downloaded into a personal computer. To allow the data to be collected over a full week, the environmental loggers were set to record every 10 seconds and the winder loggers to record every second.

Environmental loggers

The data from these loggers required some manipulation before they could be used for a meaningful comparison. The following steps had to be taken:

- 1 Calculate the wet-bulb temperature.
- 2 Ensure timing compatibility.
- 3 Calculate the measured pressure drop.
- 4 Calculate the theoretical pressure drop.

The calculation of the wet-bulb temperature does pose a challenge. The usual calculation method requires an iterative evaluation. However, the large amount of data requiring collation meant that this could not be effectively achieved. An Excel Add-In package available from kW Engineering was therefore used. This calculates the wet-bulb temperature based on data published in the 1997 *ASHRAE Handbook of Fundamentals*.

The remainder of the parameters were calculated in the usual manner, as described above.

Winders

The data for the winders are collated against time. This allows the position of the conveyance in the shaft to be calculated and these data to be synchronised with those of the data logger. To do this the specific diameter of each of the winder drums under consideration must be known. This information is then used to calculate the speed and position of the conveyances against time. Once this is

completed, 10-second snapshots of the winder movements are taken to allow comparison against the environmental data.

A typical graph showing the results of the analysis is shown in Figure 3-10.

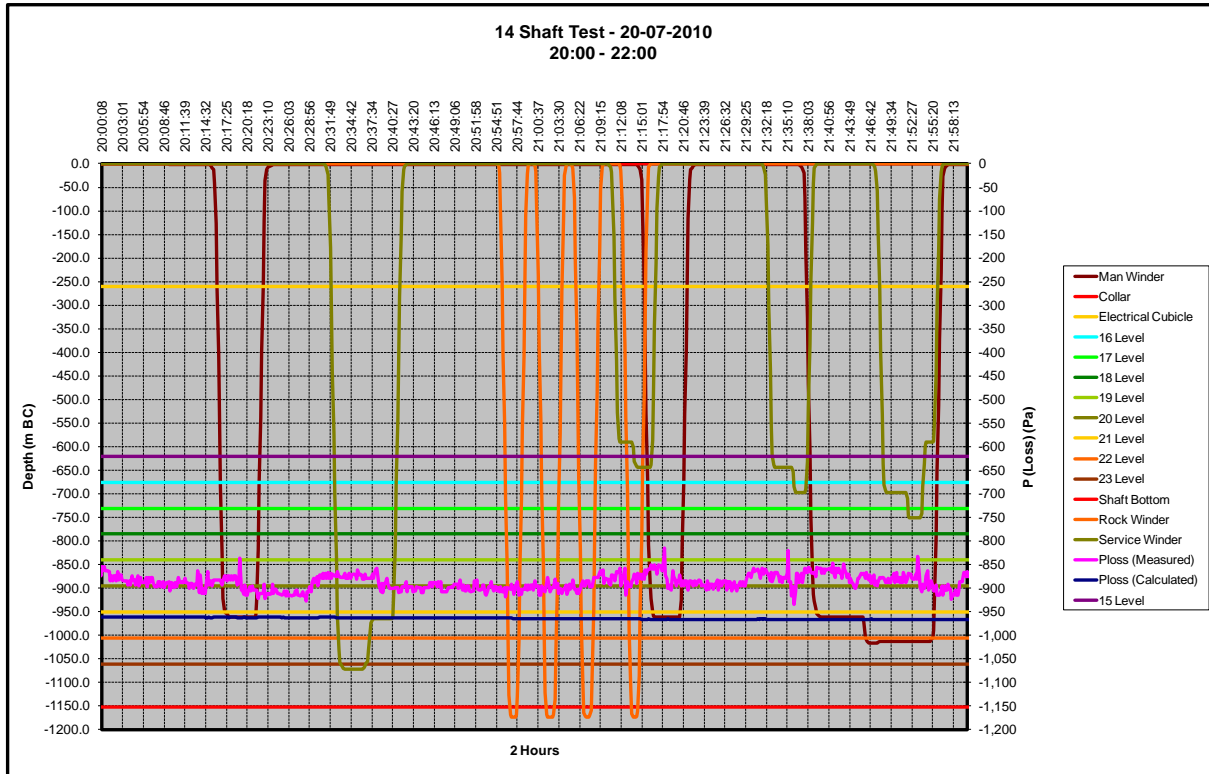


Figure 3-10: Typical graph of collated results (including environmental data and winder data)

3.5.3 Results and Conclusion

The results of the tests and the conclusions drawn from the analysis are discussed in CHAPTER 4.

3.5.4 Accuracy of Data Collation Instrumentation

The various instrumentation and loggers used for the evaluation of the various shaft systems have been discussed in the previous sections. In this section the accuracy of the measurements will be evaluated. In this evaluation, the input data to the various calculations is varied in accordance with the quoted instrument accuracy and the difference in the output is noted. The values from two points need to be considered. Thus in order to evaluate the accuracy of a measurement at two points, a total of 9 variations must be completed. These are:

- | | | |
|------|------------------------------------|-------------------------------------|
| i | Measured Value at Pt 1 | Measured Value at Pt 2 |
| ii | Measured Value at Pt 1 (+Variance) | Measured Value at Pt 2 |
| iii | Measured Value at Pt 1 (-Variance) | Measured Value at Pt 2 |
| iv | Measured Value at Pt 1 | Measured Value at Pt 2 (+ Variance) |
| v | Measured Value at Pt 1 | Measured Value at Pt 2 (- Variance) |
| vi | Measured Value at Pt 1 (+Variance) | Measured Value at Pt 2 (+ Variance) |
| vii | Measured Value at Pt 1 (+Variance) | Measured Value at Pt 2 (- Variance) |
| viii | Measured Value at Pt 1 (-Variance) | Measured Value at Pt 2 (+ Variance) |
| ix | Measured Value at Pt 1 (-Variance) | Measured Value at Pt 2 (- Variance) |

The details of the instrument used for the measurement of the temperatures and pressures in the shaft are noted in Table 3-3.

Table 3-4: Evaluation of Accuracy of Temperature Measurements on the Overall Results

Item	Temperature (Pt 1) (°C)	Temperature (Pt 2) (°C)	P _{Loss} (Difference from 1)
1	14.4	19.8	-890 Pa
2	14.7	19.8	0.6%
3	14.1	19.8	-0.6%
4	14.4	20.1	-0.6%
5	14.4	19.5	-0.6%
6	14.7	20.1	1.2%
7	14.7	19.5	-0.1%
8	14.1	20.1	0.1%
9	14.1	19.5	-1.2%

As can be seen from the above results, the accuracy of the measurement of temperature will have little effect on the overall results.

Table 3-5: Evaluation of Accuracy of Pressure Measurements on the Overall Results Typical)

Item	Pressure (Pt 1) (kPa)	Pressure (Pt 2) (kPa)	P _{Loss} (Difference from 1)
1	90.41	99.51	-890.55 Pa
2	90.51	99.51	-10.6%
3	90.31	99.51	13.4%
4	90.41	99.61	12.0%
5	90.41	99.41	-9.6%
6	90.51	99.61	-1.2%
7	90.51	99.41	-18.4%
8	90.31	99.61	-29.0%
9	90.31	99.41	-1.2%

As can be seen from the above results, the accuracy of these measurements can have the effect of increasing the calculated pressure losses by 12% or decreasing them by 29%. This relative accuracy must be borne in mind when evaluating the final results.

The details of the instrument used for the measurement of the velocity in the shaft are noted in section 3.5.1.3.

Table 3-6: Evaluation of Accuracy of the Velocity Measurements on the Overall Results Typical)

Item	Velocity (m/s)	P _{Loss} (Difference from 1)
1	9.4	-890.55 Pa
2	9.1	0.0%
3	9.7	0.0%

The free air velocity of the ventilation in the shaft was measured at various points in the shaft. This was found to be consistent along the length of the shaft. This consistency was valid as long as the no levels were passed which extracted ventilation air from the shaft.

As can be seen from the above results, the accuracy of these measurements can have the no effect on the calculated pressure losses.

3.6 COMPUTATIONAL FLUID DYNAMICS

The package used for the CFD analysis is the STAR-CCM+ from CD ADAPCO, supplied by Aerotherm in South Africa. This package allows the 3D modelling of the shaft section under consideration by solving the continuity and momentum equations inside discrete cells. The various shaft geometries were modelled in the software using the 3D-CAD module supplied. This module allows the complete model to be developed in readiness for the mesh generation.

3.6.1 Mesh Generation

The various shaft sections used in this analysis were modelled in the package using the 3D-CAD modelling features and the model was created on a 1-to-1 basis with no scaling required. This model was then meshed using a combination of the built-in polyhedral mesher for volumes and the surface remesher. The nature of the problem being examined also required that the effects of the solid interfaces and the air be modelled as accurately as possible. In this regard the Prism Layer option available as part of the meshing model was selected. This model applies additional elements at the solid interface to facilitate the accurate modelling of the turbulence around these points.

The length of the primary model section was chosen to be 20 m. However, to ensure that the flow regime within the shaft was fully developed before the pressure losses over the section were measured, the initial length of shaft to be simulated such that this flow regime could develop was 10 x the diameter of the shaft, in this instance 80 m. This required that the model be iterated four times (i.e. the output of the simulation becomes the input of the next simulation).

To ensure accurate results, a mesh refinement analysis was performed until a mesh size was found with small changes in the pressure losses. The results of this exercise are shown in Table 3-7.

Table 3-7: Mesh refinement evaluation

Base size	No. of cells in model	Reference pressure	P_{Drop} (over section)	% difference (against next value)	% of reference pressure
0.15 m	1 110 000	88 000 Pa	11.42	-5%	0.01%
0.20 m	470 000	88 000 Pa	11.74	3%	0.01%
0.25 m	350 000	88 000 Pa	11.19	15%	0.01%
0.30 m	210 000	88 000 Pa	12.87	NA	0.01%

As can be seen from Table 3-7, there is very little difference between the pressure drops measured for the mesh sizes of 0.15, 0.20 and 0.25 m.

As a result of this analysis, it was decided to use a base size of 0.25 m. This base size is sufficiently small to allow the shaft configurations to be accurately sized, but was also sufficiently large to allow the simulations to be run efficiently.

The next requirement was to determine the effect that using the prism layers would have. These layers provide additional cell data close to the skin of the cell and were thought to have an effect on the overall pressure losses over the shaft length. This setting causes the software to generate additional layers at each boundary surface, thus improving the accuracy of calculation for the surface interactions. There was, however, a negligible difference between the results from the simulations run with and without these prism layers. It was decided nonetheless to include a prism layer with a setting of 5 (i.e. five additional layers adjacent to the boundary surface) for the simulations. A schematic of the mesh arrangement is shown in Figure 3-11.

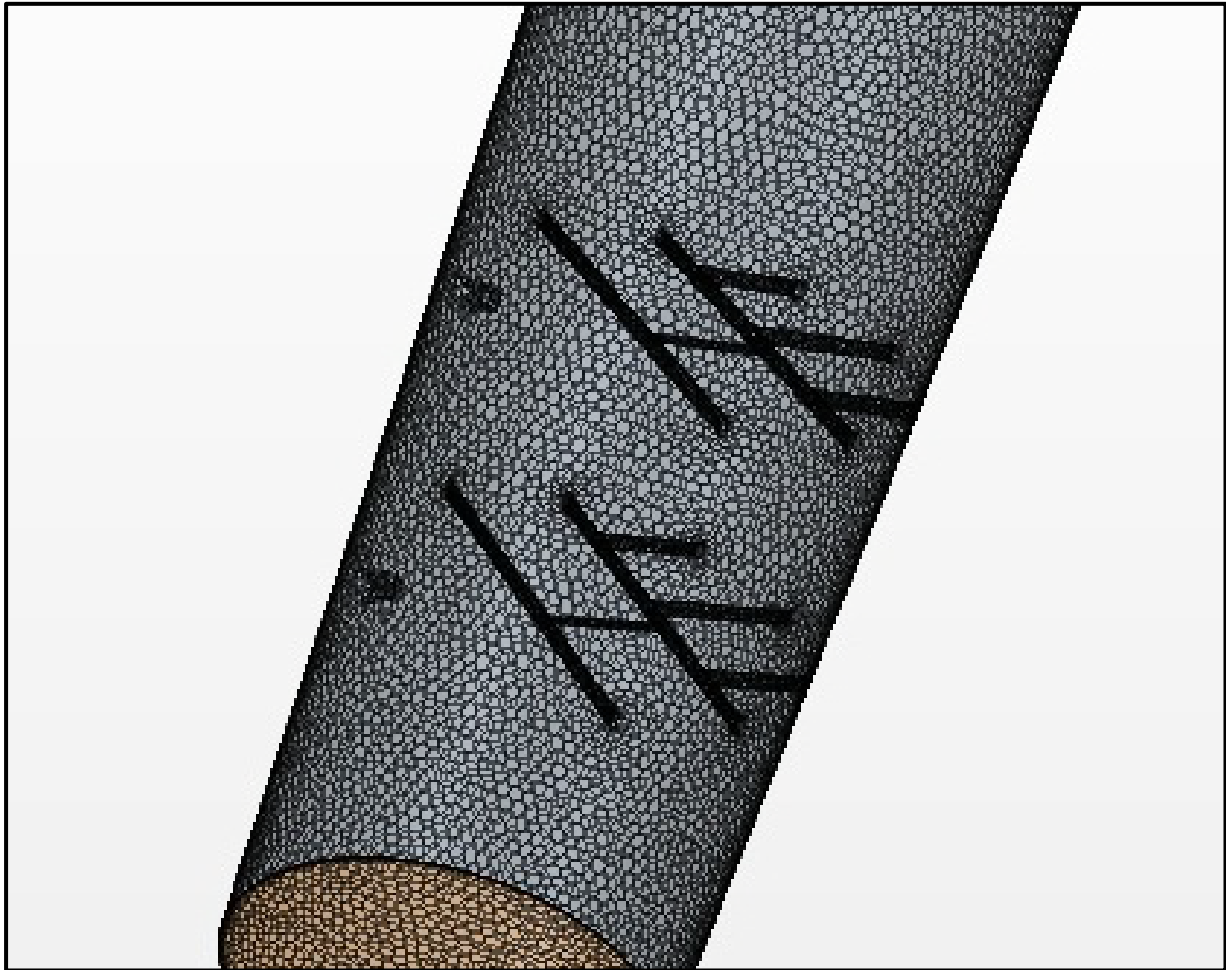


Figure 3-11: Schematic of meshed shaft arrangement

The above schematic shows a view of the mesh shaft section. Additional elements were also added to the model in accordance with the simulation requirements discussed in Section 3.6.5.

3.6.2 Fluid Model Selection

Once the geometry had been modelled and meshed, the appropriate fluid models were selected. In this instance, the thermodynamic and body forces were assumed to be small and the fluid used for the analysis was an ideal gas. The system was modelled in three dimensions and the K-Omega turbulence model was also used. These were resolved using the SIMPLE algorithm to solve the continuity and momentum equations in every cell.

The convergence requirement was set to 1×10^{-4} for continuity and momentum. This was achieved in most cases, although in some cases a convergence of 1×10^{-1} was accepted. In all instances the simulation was run until the data showed repeatability. This required that the respective curves were constant before the analysis was stopped and the results recorded.

3.6.3 Boundary Conditions

The following boundary conditions were used:

- 1 *Inlet*: The inlet was defined as a constant-velocity inlet for the first section simulated. Subsequent to this, the velocity profile used for the input was taken from the output of the previous simulation.
- 2 *Outlet*: The outlet was defined as being a constant pressure. This was consistent throughout all the simulations.
- 3 *Wall conditions*: The wall were defined as a rough wall with an asperity of 10 mm. This resulted in a Y^+ along the wall of approximately 90, which is acceptable.

It is worth noting that using the mass flow of the fluid as the input would have been ideal. However this was not possible, suffice to say the variation of the mass flow over the test section never exceeded 2.5% of the total mass flow. This is sufficiently small to not be a concern.

3.6.4 Simulation Runs

Each of the simulations was run on a personal computer running Windows XP. The computer had a hard drive with a 500 GB capacity and 4 GB of RAM. All the simulations were run using STAR-CCM+ version 6.02.007. Each simulation took between six and eight hours to complete, including all the required iterations.

3.6.5 Simulations Completed for this Analysis

To ensure a thorough understanding of the interaction between the various items contained in a shaft, it was decided to build the CFD model systematically and to include the various pieces of equipment progressively. This would allow the effect of the individual items to be evaluated. In this regard the following series of tests were completed.

3.6.5.1 T01 – Shaft barrel pressure losses

This consisted of measuring the pressure loss over a segment of the shaft barrel. Care was taken to ensure that the flow was fully developed before the results were collated.

3.6.5.2 T02 – Shaft barrel and one bunton across the shaft

This consisted of placing one bunton across the middle of the shaft in the middle of the test section. This test was used to determine the resistance that this bunton would offer to airflow through the shaft. A fully developed flow was therefore introduced at the entrance and the effect of the shaft segment evaluated.

3.6.5.3 T03 – Shaft barrel and two buntions across the shaft

This consisted of placing two buntions across the middle of the shaft at the same spacing that the buntions would normally have. This test was used to determine the resistance that the buntions would offer airflow through the shaft, including an evaluation of the interference factor that is used in the general analysis. A fully developed flow was therefore introduced at the entrance and the effect of the shaft segment evaluated.

3.6.5.4 T04 – Shaft barrel and full buntions set

This consisted of placing a full buntions set across the middle of the shaft at the same spacing that the buntions would normally have. This test was used to determine the resistance that the buntions set would offer airflow through the shaft, including an evaluation of the interference factor that is used in the general analysis. A fully developed flow was therefore introduced at the entrance and the effect of the shaft segment evaluated.

3.6.5.5 T05 – Shaft barrel and pipes at pipe diameter

This consisted of using the full shaft barrel and placing the pipes in the barrel, consistent with the normal placement and size of the pipes in the shaft under consideration. This test was used to determine the actual resistance and flow characteristics of the ventilation air around the pipes.

3.6.5.6 T06 – Shaft barrel and pipes at flange diameter

This consisted of using the full shaft barrel and placing the pipes in the barrel, consistent with the normal placement of the pipes in the shaft under consideration. The pipes were, however, modelled to have a diameter equal to that of the flanges for that pipe. This test was used to determine the actual resistance and airflow characteristics of the ventilation air around the pipes when they are modelled, as is recommended by the current theory.

3.6.5.7 T07 – Shaft barrel and pipe including flanges

This consisted of using the full shaft barrel and placing the pipes in the barrel, consistent with the normal placement of the pipes in the shaft under consideration. The pipes were modelled at the standard pipe diameter and the flanges were included at a spacing consistent with the spacing of the buntions. This test was used to determine the actual resistance and flow characteristics of the ventilation air around the pipe including the discontinuity that the flanges introduce.

3.6.5.8 T08 – Shaft barrel and buntions and pipes at pipe diameter

This consisted of using the full shaft barrel, including the buntions particular to each shaft, and placing the pipes in the shaft. These pipes were positioned consistent with the normal placement of

the pipes in the shaft under consideration.

3.6.5.9 T09 – Shaft barrel and buntions and pipes at flange diameter

This consisted of using the full shaft barrel, including the buntions particular to each shaft, and placing the pipes in the shaft, but with the pipes modelled at the same diameter as the flanges. These pipes were positioned consistent with the normal placement of pipes in the shaft under consideration.

3.6.5.10 T10 – Shaft barrel and buntions and pipe including flanges

This consisted of using the full shaft barrel, including the buntions particular to each shaft, and placing the pipes in the shaft. The pipes were modelled at the standard pipe diameter and the flanges were included at a spacing consistent with the spacing of the buntions. These pipes were positioned consistent with the normal placement of pipes in the shaft under consideration.

3.6.5.11 T11 – Shaft barrel and buntions and pipe including flanges and skip 1

The full shaft barrel was modelled, including all the buntions and pipes. The skip in this instance was modelled in position in the shaft.

3.6.5.12 T12 – Shaft barrel and buntions and pipe including flanges and skip 2

The full shaft barrel was modelled, including all the buntions and pipes. The skip in this instance was modelled in position in the shaft.

3.6.5.13 T13 – Shaft barrel and buntions and pipe including flanges and man cage 1

The full shaft barrel was modelled, including all buntions and pipes. The man cage in this instance was modelled in position in the shaft.

3.6.5.14 T14 – Shaft barrel and buntions and pipe including flanges and man cage 2

The full shaft barrel was modelled, including all the buntions and pipes. The man cage in this instance was modelled in position in the shaft.

3.6.5.15 T15 – Shaft barrel and buntions and pipe including flanges and service cage

The full shaft barrel was modelled, including all the buntions and pipes. The service cage in this instance was modelled in position in the shaft.

3.7 ECONOMICS

The emphasis of the work reported on in this thesis was on comparing the overall lifecycle cost of different equipping options and the associated capital costs to elicit a total cost for the life of mine (LOM).

The basis for this comparison was 20 years at a lower-than-anticipated electrical tariff increase of 10% per annum.

3.7.1 Shaft Modifications

This was not evaluated in detail for the reasons discussed in Section 1.5.1. The costs associated with the different diameters are shown in Figure 1-11.

3.7.2 Shaft Equipping

This refers to the potential modifications to the steelwork and fittings in the shaft. Such modifications can be classified into three sections:

- 1 *Shaft steelwork:* These are the buntons and the guides that are used to guide the shaft cages and skips while they are traversing the shaft. The cost of the shaft steelwork will be based on a R/m basis. The potential increase or decrease in this value was evaluated against recent data obtained for the equipping of shafts.
- 2 *Installation time:* Discussions with shaft-sinking professionals showed that the installation times for the various buntion configurations are sufficiently similar to ensure that these costs will be the same whatever the shape.
- 3 *Shaft service:* The requirement of the shaft services (i.e. piping, cables, etc.) is defined by the mining operations and is beyond the purview of this work. However, the placement of these items in the shaft in order to optimise the pressure losses in the shaft is within the scope of this work. The installation time for these should be the same no matter where they are installed around the shaft circumference. This will, however, be reviewed and any potential differences between the capital costs will be evaluated in a similar manner to that described in points 1 and 2 above.

3.7.3 Shaft Conveyances

This evaluation will pertain primarily to the slight modifications that can be made to the conveyances which will potentially give the largest savings.

3.7.4 Operating Costs

These costs are generally the most difficult to evaluate. However, most shaft maintenance activities are completed during the legally required shaft inspections. These inspections are carried out weekly, and it is during this time that the general cleaning and basic maintenance work is carried out.

Generally, any additional work required on the shaft results from external factors or activities, e.g. corrosion, pipe misalignment due to impact from a falling object, steelwork alignment due to long use, etc. It is therefore appropriate to derive the operating costs of the shafts from the electrical requirement to transfer the ventilation air through the shaft. Thus a pressure and flow requirement for the shaft will be calculated and the electrical costs required to deliver this pressure and flow will be calculated.

It is not possible to compare the specific costs associated with each shaft as this is dependent on variables specific to that shaft, e.g. the transmission zone. The transmission zones are the zones into which Eskom has divided the country to allow for a cost associated with the supplying of a specific geographical location. The calculation will therefore be made from the MEGAFLEX (non-local authority rate) as supplied in the Eskom 2011 Tariff book (Eskom, 2011). These costs and the assumptions used for the calculation are listed below:

- 1 Transmission zone – Assumed to be ≥ 600 km and ≤ 900 km
- 2 Voltage – ≥ 500 V ≤ 66 kV
- 3 Charges will be calculated excluding VAT
- 4 Assumed to be a key customer
- 5 Equipment will be assumed to be running 24 hours a day, 7 days a week, for comparative reasons.

3.8 SUMMARY OF METHOD OF EXPERIMENTATION AND ANALYSIS

The objectives of the work presented in this chapter were the following:

- 1 Present the current theory used for the evaluation of pressure drops in shafts.
- 2 Define a methodology for the testing of working shafts to validate this theory.
- 3 Define the CFD analysis techniques to be used for the evaluation of the shafts.
- 4 Define the method by which the economic evaluation of the shaft systems will be carried out.

The current theory for the evaluation of shaft resistances is based on a mix between the standard fluid dynamics Chezy-Darcy friction factor theory for duct flow, an extrapolation of drag coefficients for various buntion shapes and an extrapolation of data for the resistance that shaft conveyances offer when moving in a shaft. The resistances offered to the ventilation flow by the buntions, guides, shaft fittings and rough surface of the shaft wall are all calculated separately. These resistances are reduced to a value of the standard Chezy-Darcy friction factor (f). This factor is then applied to the standard fluid dynamics equation for the calculation of friction losses in ducts.

The pressure loss resulting from the movement of a conveyance in the shaft is calculated separately from the empirical data. This pressure loss is then added to or subtracted from the shaft pressure losses calculated from fluid dynamic theory depending on the direction in which the conveyance is travelling.

To validate the current theory, it was necessary to complete tests on working shafts. These were conducted on Impala Platinum shafts. A methodology for the additional dynamic tests on the shafts was presented in this chapter. This included the use of loggers to ensure that the ventilation response to the use of conveyances is understood. Measurement devices were installed in the shaft at appropriate intervals. These results were collated with those from the rotary encoders that were placed on the winder in order to determine the position of the conveyances in the shaft. The combination of these results gave the standard resistance of the shaft when the conveyances were stationary as well as when they were moving. The results of this analysis are discussed in CHAPTER 4.

Once the analysis had been completed and the general verification of these shafts against the current theory had been done, the next phase of the work was to model the shaft. This was done to try and gain an understanding of the various items in the shaft and the resistance they offer to the ventilation flow. For this purpose computational fluid dynamic (CFD) analysis was used. This analysis was completed using the STAR-CCM+ package. Various CFD models were evaluated, with specific emphasis on building the models by introducing the various items in the shaft into subsequent models. The purpose was to determine the effect that each of these items had on the overall resistance that the buntions and fittings offered to the ventilation flow.

The goal of the analysis presented in this thesis is to find ways in which to reduce the resistance the shaft offers to ventilation flow through it. In this regard, it is important to evaluate the potential solutions in order to determine the savings that could be achieved. To do this, the effect of various modifications was evaluated against the reduced operating and capital costs for those modifications. These costs were calculated from the Eskom 2011 Tariff book.